NEW COMPARISONS BETWEEN FRESH IMPACT CRATERS ON MERCURY AND THE MOON.

Zhiyong Xiao[1,2], Robert G. Strom[1], Clark R. Chapman[3], and James W. Head[4]. [1]Lunar and Planetary Laboratory, University of Arizona, Tucson, AZ 85719, USA, xiaobear@lpl.arizona.edu. [2]Faculty of Earth Sciences, China University of Geosciences (Wuhan), Wuhan, Hubei 430074, P.R.China. [3]Department of Space Sciences, Southwest Research Institute, Boulder, CO 80302, USA. [4]Department of Geological Sciences, Brown University, Providence, RI 20912, USA.

Introduction: The morphology of fresh impact craters and the distribution of their secondaries are windows into the study of factors affecting the impact cratering process, such as surface gravitational acceleration, target lithology, and impact velocity. Impacts on airless bodies, such as Mercury and the Moon, are ideal laboratories for comparative studies of impact processes. Earlier studies about this issue used Mariner 10 data for mercurian craters [1,2,3]. Due to the limited image resolution and coverage of Mariner 10 data, earlier studies of Mercury included few craters [2]. High-resolution images under optimum Sun angles, now being obtained by the Mercury Dual Imaging System (MDIS) during the primary orbital phase of the MESSENGER mission, allow detailed morphologic comparisons between craters on the Moon and Mercury.

Research Method: Global mosaics from the Lunar Reconnaissance Orbiter Camera Wide Angle Camera (100 m/pixel) and images from MDIS (250 m/pixel on average) are used in this study [4, 5]. Copernican craters on the Moon and Mansurian craters on Mercury, both from the diameter range ~20-300 km, were selected for this study.

Fresh impact craters are divided into four circumferential areas: crater interior, continuous ejecta deposit facies, continuous secondaries facies, and discontinuous secondaries facies (Fig. 1). Few projectiles impact vertically. Therefore, although parent craters are circular in shape, the distribution of their impact ejecta is seldom axially symmetric about the surface normal to the impact point [6]. In this study, we measured the surface areas instead of radial distances to represent the scales of the continuous ejecta deposit facies (S1) and continuous secondaries facies (S2). The average radial extents (L1 and L2) were calculated for these respective deposits. We also measured the diameter of the largest secondary crater (d_{max}) on the continuous secondaries facies for each crater, and we compared the crater size-frequency distribution of secondaries on the continuous secondaries facies for similar sized lunar and Mercury craters.

Results: For a given crater diameter *D*, S2 is similar for craters on the Moon and Mercury, but S1 for lunar craters is larger by a factor of ~1.25 (Fig. 2A). Similar results are seen when the comparison is made between *D* and L1 or L2 (Fig. 2B).

On Mercury d_{max} is about 1.2 to 2.5 times larger than that for similar sized lunar craters (Fig. 3). We compared the size-frequency distribution of secondaries on the continuous secondaries facies of the lunar crater Copernicus (93 km diameter) and craters Hokusai (114 km) and Abedin (116 km) on Mercury. Their crater size-frequency distribution curves all have steep slopes, and the steep segments are subparallel to each other (Fig.3B).

We found that a large number of Mercury craters have circular and isolated secondaries on the continuous secondaries facies, especially for large impact basins. In contrast, secondaries on the Moon are highly irregular in shape and occur mostly in clusters or chains [7]. Only the Orientale basin has similar circular and relatively isolated secondaries on the Moon.

Discussion and Conclusion: Some of our findings confirm previous observations, which were ascribed to the larger surface gravitational acceleration on Mercury [1, 2]. For example, Mercury craters have smaller continuous ejecta deposits and Abendin has higher crater densities of secondaries on the continuous secondaries facies than Copernicus. However, most of the results cannot be solely explained by the differences in gravitational acceleration [8].

From this study, along with impact cratering mechanics analysis and analog studies, several generalizations may be made:

1. Mercury's larger surface gravitational acceleration restricts the range of continuous ejecta deposit facies around impact craters of a given size.
2. Craters on Mercury have larger ejection velocities than similar sized lunar craters. Therefore, their continuous secondaries facies are more widespread and the spatial densities of secondaries is lower.
3. The large span of impact velocities on Mercury greatly affects the sizes and spatial density of secondaries relative to the Moon.

References: [1] Gault, D. E. et al. (1975), *JGR*, 80, 2444-2460. [2] Schultz, P. H., and J. Singer (1980), *Proc. Lunar Planet. Sci. Conf. 11th*, 2243-2259. [3] Villas, F., et al. (*ed.*) (1989), *Univ. Ariz.*, pp 165-335. [4] Robinson, M.S. et al. (2008), *LPS*, 40, 1576. [5] Hawkins, S. E., III, et al. (2007), *Space. Sci. Rev.*, 131, 247-338. [6] Richardson, J. E. et al. (2007), *Icarus*, 190, 357-390. [7] Oberbeck, V. R., and R. H. Morrison (1974), *Moon*, 9, 415-455. [8] Cintala, M. J., et al. (1977), *Proc. Lunar Sci. Conf. 8th*, 3409-3425.

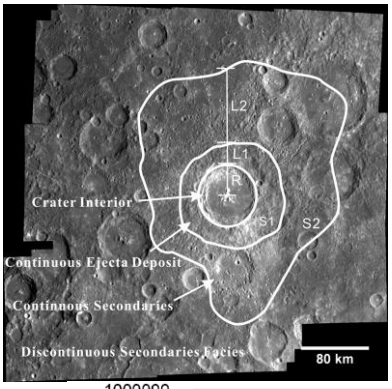

Fig. 1. Example circumferential areas for an unnamed Mercury crater centered at 0.71°S, 251.65°E. The base mosaic is from MDIS images EN0211413816M, EN0211413818M, EN0211414071M, EN0211414073M, N0211457281M, EN0211457283M, EN0211457535, EN0211457752M, EN0211457754M, EN0211500758M, EN0211500760M,EN0211501016M, EN0211501018M, EN0211501230M, EN0211544488M,EN0211587687M, EN0211587940M, EN0211588153M, EN0211588155M, EN0211631602M, and EN0211674615M. North is up. On planetary surfaces, few impact craters have symmetric distributions of continuous ejecta deposit or continuous secondaries facies. We used surface areas (S1 and S2) instead of radial distances to represent the scales for these terrains. R is the average radius of the crater rim, and L1 and L2 are the average radial extents of S1 and S2, respectively.

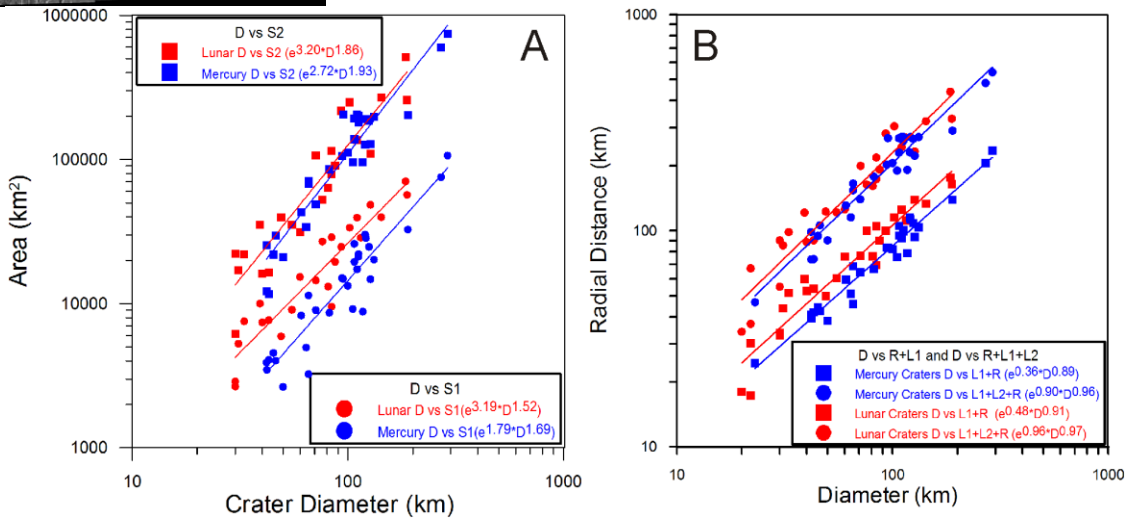

Fig. 2. (A) Comparison of S1 (dots) and S2 (squares) between craters on Mercury (blue) and the Moon (red). S1 for lunar craters is larger than that for similar sized Mercury craters, but S2 is similar. (B) Comparison of the averaged radial distances from crater centers to the outermost continuous ejecta deposit (R+L1, squares) and those to the outermost continuous secondaries facies (R+L1+L2, squares) for lunar (red) and Mercury craters (blue). Relations between crater diameter (*D*) and S1, S2, L1, L2, L1+R, and R+L1+L2 (X) are fit by power laws of the form $X = a * D^b$, where a and b are constants. All the figures are log-log plots.

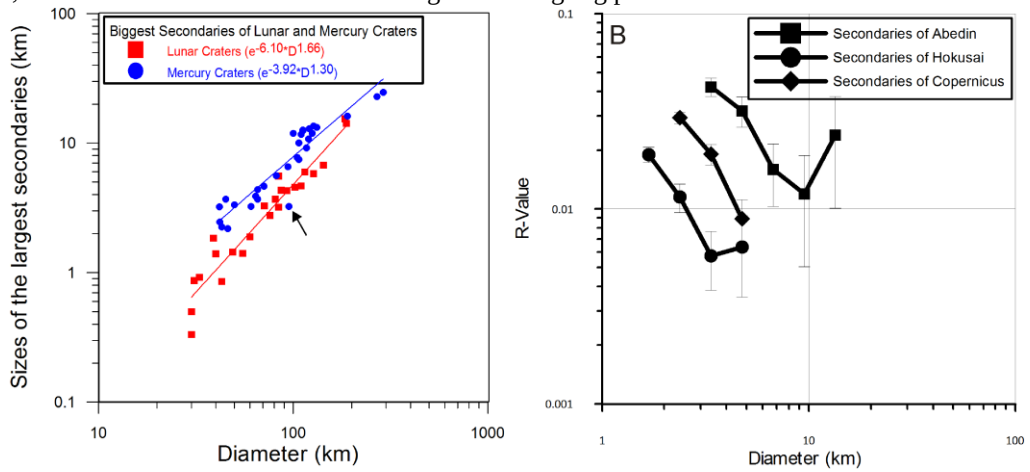

Fig. 3. (A) Comparison of d_{max} for craters on the Moon (red squares) and Mercury (blue dots). The black arrow indicates d_{max} for Hokusai crater, which is below the average level, perhaps because of a greater impact velocity. Relations between *D* and d_{max} (straight lines) are of the form $d_{max} = a * D^b$, where a and b are constants. (B) R plot of the size-frequency distributions of secondaries on the continuous secondaries facies of Copernicus crater on the Moon (diamonds) and the craters Abedin (squares) and Hokusai (dots) on Mercury.